MM Science Journal | www.mmscience.eu
ISSN 1803-1269 (Print) | ISSN 1805-0476 (On-line)
Special Issue | HSM 2025
18th International Conference on High Speed Machining
October 15-16, 2025, Metz, France
DOI: 10.17973/MMSJ.2025_12_2025159

HSM2025-44839

NOVEL APPROACH TO DOSING CARBON DIOXIDE BASED CRYOGENIC MINIMUM QUANTITY LUBRICATION BY HIGH-FREQUENCY PULSED APPLICATION

J. H. Selzam[1]*, P. Binner[1], T. Meier[1], N. Hanenkamp[1]

[1]Friedrich-Alexander-University Erlangen-Nuremberg, Institute for Resource and Energy Efficient Production Systems, Fuerth, Germany

*Corresponding author; e-mail: jan.selzam@fau.de

Abstract

Carbon dioxide (CO_2) based cryogenic minimum quantity lubrication (cMQL) is an alternative approach to facilitate cooling lubrication of cutting processes. While it offers greater sustainability than conventional metalworking fluids (MWF), its precise, process-specific dosing can be challenging. This is due to the physical properties of the pressurized CO_2, as it already develops its cooling effect in the supply line if expanding there. The paper therefore proposes a new approach to the dosing of this coolant strategy which is based on high-frequency pulsed application. By opening and closing a valve in the immediate vicinity of the application nozzle at high frequency, a precisely adjustable fraction of the maximum mass flow can be directed to the cutting zone. This allows the cooling capacity to be adjusted accurately and adapted to the process. In addition, the proposed setup makes it possible to react to the fluctuating input quality of the CO_2. This paper examines how accurately the mass flow can be dosed using high-frequency CO_2 pulses. It also investigates whether continuous and pulsed cMQL have comparable cooling capacities at the same mass flow rate and to what extend the input quality of the CO_2 can be compensated.

Keywords:

Cryogenic cooling, pulsed coolant application, adaptive dosing

1 INTRODUCTION

Wet machining is the industry standard for metal cutting. In over 90 % of all applications, conventional MWF are supplied to the workpiece in the form of flood or high-pressure cooling [Denkena 2011]. Although this type of process cooling is functional, it is not very sustainable. One of the main points of criticism is the high consumption of media, some of which are harmful to human health and the environment [Najiha 2016]. Even if attempts are made to operate the MWF in a closed circuit, large quantities are lost over time through evaporation, vaporisation and drag-out.

An alternative cooling lubrication strategy that can also be used for demanding machining tasks and uses fewer media is cMQL [Gross 2021]. It combines the cooling effect of cryogenic media, such as CO_2 or liquid nitrogen (LN_2), with the lubricating effect of minimum quantity lubrication (MQL). As LN_2 is always cryogenic, it poses challenges in terms of storage, supply and its mixing with oil. CO_2 on the other hand can be stored and supplied at room temperature at a pressure of $p = 59$ bar. This also means that oil can be added to liquid CO_2, so that both can be supplied together. The CO_2-oil mixture only cools down to cryogenic temperatures during expansion due to the Joule-Thomson effect. This reduces the integration effort and thus simplifies implementation in industrial series processes and machines.

As mentioned earlier, CO_2-based cMQL has not yet been widely adopted, despite its advantages. One possible reason for this is that the system technology is not yet fully developed, which is also due to the relative novelty of this approach. Precise dosing of the cMQL is particularly difficult due to the physical properties of CO_2. As the CO_2 is only allowed to expand at the cutting zone, the use of throttles is not possible. This dampens the sustainability benefits of cMQL compared to conventional cooling lubrication strategies and makes the topic of process-specific dosing one of the focal points of research in this field [Meier 2024].

The high-frequency pulsed application of cMQL (HFpcMQL) represents a novel and promising approach. The high-frequency opening and closing of the outlet valve is intended to direct a precisely adjustable fraction of the maximum mass flow to the cutting zone. Doing so, the cooling capacity and lubrication performance can be selected depending on the cutting process. Furthermore, this approach makes it possible to react to the fluctuating quality of the CO_2 supply, which allows for processes that are more robust. Therefore, this paper investigates the dosing precision for the mass flow of CO_2 and its cooling capacity as well as the application pattern of the lubrication oil with HFpcMQL and compares the results continuously with continuous cMQL.

2 STATE OF THE ART

The main tasks of MWF, also known as cooling lubricants, in the machining process are the cooling and lubrication of the cutting zone and the removal of chips from it. These MWF, which are usually oil- or water-based, are supplied to the cutting zone in the form of flood or high-pressure cooling from the outside or through cooling channels in the tool. Conventional cooling lubricants, which are often composed of mineral oils and additives, contribute significantly to the high performance level of modern production processes [Klocke 2008]. However, this also gives rise to some negative aspects that affect all three dimensions of sustainability [Najiha 2016]. High costs are incurred for the procurement, maintenance and, above all, disposal of conventional cooling lubricants. In addition, MWF endanger people [NIOSH 1998] and the environment [Howes 1991] through leaks, drag-out losses and other types of emissions. [Kißler 2004]

In order to reduce these economic, ecological and social consequences, numerous approaches have already been developed to minimize the use of cooling lubricants. For example, MQL and dry machining are already being used in industry alongside conventional flood cooling lubrication [Degner 2019]. Yet both strategies quickly reach their limits, especially when machining difficult-to-cut materials [Pimenov 2024].

One option to counteract the thermo-mechanical stress on the tool in the cutting zone is the use of cryogenic cooling. Research into cryogenic cooling based on LN_2 was particularly advanced at the turn of the millennium. A study by *Hong and Broomer* shows that cryogenic machining of AISI 304 with LN_2 and targeted cooling of the rake face can increase tool life by up to 67 % compared to emulsion cooling. Cryogenic cooling proved to be particularly effective at higher cutting speeds. Excessive cooling of the major and minor cutting edges, on the other hand, led to premature tool failure [Hong 2000]. *Wang and Rajurkar* use a closed-loop system with LN_2 to specifically cool the cutting edges when turning high-performance materials such as titanium alloys, Inconel 718 and tantalum. The study shows that the resulting reduction in tool and workpiece temperature leads to increased tool life and improved surface quality compared to MWF [Wang 2000].

However, due to the low boiling point of ϑ = -196 °C, the storage and handling of LN_2 is very complex. CO_2, on the other hand, can be stored in liquid form at a pressure of p = 59 bar and room temperature in riser bottles, which makes handling and integration into the machine system much easier. After the liquefied CO_2 has been supplied to the cutting zone through the corresponding pipe system, it expands there due to the pressure drop at the nozzle outlet. The liquid CO_2 evaporates and cools down due to the Joule-Thomson effect. The amount of heat required for the phase conversion is so great that cooling to approximately ϑ = -78 °C occurs. One further advantage of both LN_2 and CO_2 is that these cooling media evaporate completely after use and leave no residue on the workpiece, the chips or the machine tool. In the experiments conducted by *Jerold and Kumar*, CO_2 cooling enabled effective temperature control when turning AISI 316 compared to wet and dry machining. This significantly reduced cutting forces, decreased tool wear and improved surface quality. Particularly at high cutting speeds, cryogenic cooling also has advantages in terms of chip breaking behaviour and process stability [Jerold 2012]. *Gupta et al.* investigated tool wear when turning aluminium 024-T351 under different cooling lubrication strategies with constant cutting parameters. Compared to dry and MQL machining, CO_2 cooling showed a significantly lower level of flank wear and crater wear as well as a more uniform wear pattern at the tool tip [Gupta 2023].

In order to ensure effective lubrication of the cutting process in addition to cooling, cryogenic cooling was combined with MQL in the cMQL. This combination further improves the results achieved with purely cryogenic cooling. *Biermann et al.* showed that during the turning of Ti6Al4V, pure CO_2 cooling already resulted in less tool wear than flood cooling. However, when machining Ti6Al2Sn4Zr6Mo, CO_2 cooling alone did not lead to a longer tool life. Only the combined application in the form of cMQL led to an increase in tool life of around 25 % due to reduced friction at the cutting edge [Biermann 2015]. *Hanenkamp et al.* developed their own system for cMQL in which the liquid CO_2 is combined with lubricating oil via an HPLC pump in order to minimize the integration effort. Milling tests were carried out on Ti6Al4V for evaluation and compared with conventional MWF. The results showed reduced cutting forces and improved surface quality when using suitable lubricants such as ester oils and fatty acid alcohols [Hanenkamp 2018]. In the study by *Villarrazo et al.*, the influence of cMQL when using CO_2 was investigated in comparison to conventional MQL when milling AISI 1045. Despite comparable cutting forces, a significant increase in tool life and an increase in cutting speed was achieved through the use of cMQL. In addition, cMQL showed a more homogeneous wear behaviour, while the tendency to adhesion on the cutting edge was significantly reduced compared to MQL [Villarrazo 2023]. To get an insight into the current state of development of cMQL, *Iruj et al.* have created a comprehensive overview [Iruj 2024].

Even though cMQL has clear advantages over other cooling lubrication strategies, particularly when machining difficult-to-cut materials, there are only limited possibilities for implementing flexible, process-specific dosing. The most frequently chosen approach is the use of nozzles with different diameters [Bagherzadeh 2018]. Although this permits simple system technology, it only allows discrete values to be approached, which also depend on the input quality of the CO_2. In addition, it is not yet possible to change the nozzle quickly, which makes it even more difficult to use in industrial production. Another approach is the use of supercritical CO_2 ($scCO_2$). Although this enables variable dosing, additional effort is required to keep the CO_2 in the entire supply system safely in a supercritical state (ϑ > 31.0 °C, p > 73.8 bar) [Stephenson 2014].

An approach that has also been used recently is the dosing of cMQL by pulsed application. This involves periodically opening and closing a valve in order to feed a fraction of the maximum mass flow to the cutting zone. *Iqbal et al.* carried out the first investigations into the milling of Incoloy 825 using pulsed cMQL (pcMQL) with CO_2 in 2023. A pulse frequency of f_p = 0.5 Hz was used. Compared to continuous application, pcMQL resulted in improved surface quality and a slight reduction in cutting forces at higher cutting speeds. The continuous cMQL, on the other hand, proved to be more advantageous in terms of tool wear. In addition, the study demonstrated the potential for reducing the consumption of cryogenic medium through pulsed application [Iqbal 2023]. In a second study *Iqbal et al.* examined the influence of pcMQL on further nickel-based alloys. This time the pcMQL proved to be at least on par with continuous cMQL in terms of flank wear [Iqbal 2024]. Similar experiments on pcMQL were carried out by *Naik and Sharma* using LN_2. They obtained comparable results, but were also able to demonstrate that a higher pulse frequency yields better overall results [Naik 2023].

As these studies show, pulsation can be used as a means of dosing. In addition, it is shown that a higher pulse frequency has an altogether favourable effect on process characteristics such as tool life, surface quality and cutting forces. However, in the studies cited, the maximum output is only ever halved at low pulsation frequencies. A targeted control of the media flow and thus the cooling and lubrication performance is not pursued.

In order to further improve the results achieved to date with pulsation, the pulse frequency is significantly increased in this paper. Furthermore, the aim is to set freely selectable fractions of the maximum mass flow and thus the cooling capacity by varying the opening and closing times of the application valve. Instead of a specific process, the focus of this study is on the fundamentals and system technology.

3 EXPERIMENTAL SETUP AND DESIGN

3.1 Experimental setup

For the systematic investigation of CO_2-based HFpcMQL, the experiments are carried out in two parts and in separate setups. In the first part, experiments are conducted to measure the mass flow of the CO_2 carrier medium and its cooling capacity. In the second part, the spray pattern of the pulsed oil application is investigated.

The schematic experimental setup for the first part of the experiments is shown in Fig. 1. The CO_2 is stored in a riser bottle bundle at room temperature and a pressure of p = 59 bar. To ensure a reliable and constant supply of CO_2, a pre-cooler can be integrated into the experimental setup. Pre-cooling can increase the liquid content of the CO_2, which increases its density [Meier 2024].

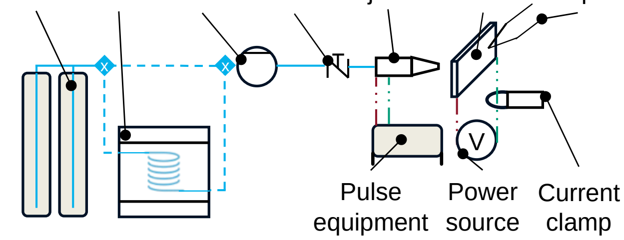

Fig. 1: Setup for the measurement of mass flow and cooling capacity of CO_2.

A Coriolis sensor is used to measure the mass flow and density of the CO_2. Two smooth jet nozzles with diameters of d = 0.2 mm and d = 0.3 mm are used for the continuous CO_2 supply, which serves as a reference in all experiments. The pulsed supply of CO_2 is achieved using two modified electromagnetic fuel injectors of the type Bosch HDEV5. This type of injector has already been used successfully for the pulsed supply of CO_2 in previous studies. For this paper, the regular injection nozzles of the two injectors were closed by laser powder deposition welding in order to subsequently create a new central bore in each case. One injector with a nozzle diameter of d = 0.5 mm and one injector with a nozzle diameter of d = 1.0 mm were produced. The injectors are controlled in a two-stage process. The trigger signal with the desired frequency is generated by a microcontroller. This signal is then fed to the trigger input of a pulse shape generator, which outputs a pulse signal to the injector. Fig. 2 shows the idealised current curve of such a pulse signal and the corresponding valve displacement response of the injector. The valve displacement of the injector provides a good approximation of the mass flow. In order to open the injector as fast as possible, a boost current I_b is applied for a short time in the beginning of each pulse. The duration of this boost time t_b is selected so that the injector is reliably open after t_b has elapsed. The duration therefore depends primarily on the injector system. After the boost time t_b has elapsed, the current is reduced to the holding current I_h. This is chosen to be high enough to keep the injector open and low enough not to overload it thermally. The duration of the holding current is freely selectable and can therefore be used to influence the application time of the media. At the end of the holding time, the injector is de-energised and closed by an integral spring.

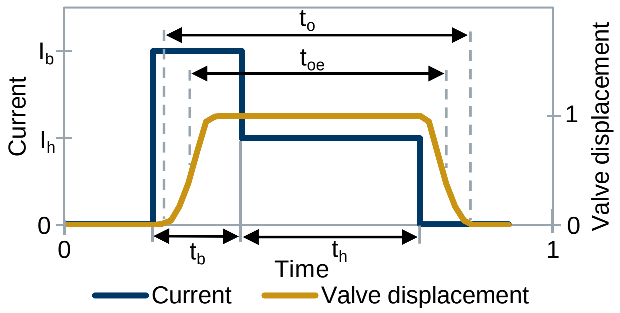

Fig. 2: Idealised current and displacement curves of an electromagnetic injector.

The pulsation is used to dose the mass flow. As the injector is safely open during the holding time, it is assumed for a first characterisation step that the fraction of the maximum mass flow $\dot{m}_f$ is a function of the maximum mass flow $\dot{m}_{max}$, the pulse frequency f_p and the holding time t_h:

$$\dot{m}_f = \dot{m}_{max} \cdot f_p \cdot t_h \quad (1)$$

In reality, however, the injector is already at least partially open before the start of the holding time and after the end of the holding time, as can be seen in Fig. 2. Therefore, the actual pulse duration t_o exceeds the set holding time t_h. For the following correction model, the equivalent pulse duration t_{oe} is introduced as an auxiliary variable in which the injector is mathematically fully open. It exceeds t_h by a difference of Δt:

$$t_{oe} = t_h + \Delta t \quad (2)$$

To correct for this difference, the original formula is extended and the correction factor Δt for the used injectors is determined in the course of the paper:

$$\dot{m}_f = \dot{m}_{max} \cdot f_p \cdot (t_h + \Delta t) \quad (3)$$

To measure the cooling capacity $P_{Cooling}$, the CO_2 jet is directed onto a heating resistor. This heating resistor is supplied by a constant 24 V power source and regulates its power consumption according to its temperature. As a result, the electrical current increases as soon as the heating resistor is cooled down, for example with CO_2. The required current is measured using an RS CP-10 current clamp and used to calculate the power consumption for heating $P_{Heating}$, after equilibrium has been reached. As the heating resistor requires a constant basic power P_{Stable}, this must be subtracted from the measured heating power $P_{Heating}$ to obtain the corresponding cooling power $P_{Cooling}$, shown in Formula (4). In the following chapters, only the actual cooling capacity $P_{Cooling}$ = P_c is specified.

$$P_{Cooling} = P_{Heating} - P_{Stable} \quad (4)$$

In addition to the cooling capacity, the temperature at the heating resistor is measured using a type k thermocouple. This setup is a further development of the setup used by *Meier et al.* to measure the cooling capacity [Meier 2024]. An overview of the setup-specific parameters is provided in Tab. 1. It contains information on the nozzle and its distance to the targets, the pre-cooling temperature and the heating resistor.

Tab. 1: Setup-specific parameters.

Dimension	Values
Smooth jet nozzle diameter d (mm)	0.2, 0.3
Injector nozzle diameter d (mm)	0.5, 1.0
Nozzle distance to target (mm)	40
CO_2 pre-cooling temperature (°C)	~ 9.5
Heating panel dimensions (mm)	75 x 25
Heating panel current (V)	24

In order to consider the cMQL as a whole, the second part of the experiments analyses the oil output. The experimental setup, shown in Fig. 3 is partially analogous to that in Fig. 1. CO_2-bundle, pre-cooler, Coriolis sensor and shut-off valve are set up as previously.

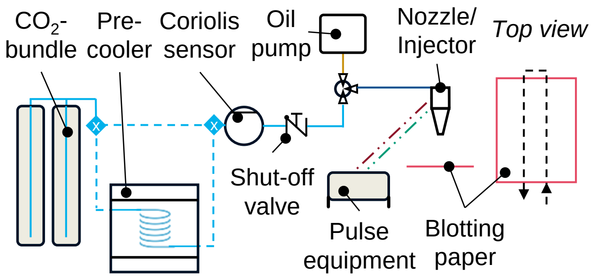

Fig. 3: Setup for the examination of oil output.

After the valve, oil is added to the CO_2 via an HPLC pump. The combined CO_2-oil mixture is then fed to the smooth jet nozzle or injector. If an injector is used, it is controlled in the same way as in the previous experiments. During the application of the media mixture, the injector or smooth jet nozzle is moved by a milling machine over blotting paper. In order to obtain meaningful results for the oil output, the mass applied, the path width and the spray pattern are analysed. To determine the mass, the blotting paper sheets are weighed immediately before and after the media application using a precision scale, while the path width and spray pattern are analysed using images with a length standard.

3.2 Experimental design

The aim of this research is to enable precise dosing of CO_2-based cMQL for cutting operations in terms of mass flow, cooling capacity and oil application by means of high-frequency pulsation. The pulsation should allow a freely selectable fraction of the maximum mass flow to be set.

Therefore, the first step is to determine the maximum mass flow with continuous CO_2 supply for two smooth jet nozzles and two modified fuel injectors. The smooth jet nozzles with diameters of $d = 0.2$ mm and $d = 0.3$ mm have already been used several times in previous research work and serve as a reference [Gross 2021]. The two injectors, which will later be used to implement the high-frequency pulsation, have bore diameters of $d = 0.5$ mm and $d = 1.0$ mm. As explained in the previous chapter, the maximum cooling capacity occurring on a heating resistor is also measured during the determination of the maximum mass flow. In order to account for the input quality of the CO_2, the experiments are carried out with CO_2 at room temperature and pre-cooled CO_2 with higher density.

Based on the results of the first experiments, in a second step the injector with $d = 0.5$ mm is pulsed in such a way that the same calculated mass flow is achieved as with the two smooth jet nozzles. In this first step the characterisation Formula (1) is used. This is done at the three frequencies $f_p = 50 / 100 / 150$ Hz and the corresponding holding times t_h. These experiments are also carried out with and without pre-cooling. Once again, both the mass flow and the cooling capacity are recorded. By comparing the results of continuous and pulsed application, the initial dosing precision of the system can be estimated.

In order to further improve the dosing precision, a mathematical correction is performed using the data from the previous experiments. As already explained in chapter 3.1, the time during which the injector is at least partially open t_o exceeds the set holding time t_h, as shown in Formula (2). This discrepancy Δt can be estimated with the previously collected data and used as a correction factor for further experiments. To obtain a result as meaningful as possible, data for all three frequencies with corresponding holding times and both with and without pre-cooling are used for this purpose.

Once the correction factor has been determined, it is tested by means of validation experiments. For this purpose, the mass flows $\dot{m} = 5$ kg/h and $\dot{m} = 10$ kg/h are specifically approached with the pulse frequencies $f_p = 50 / 150$ Hz and the corresponding holding times using the injector with the nozzle diameter $d = 0.5$ mm. The aim is to check to what extent the dosing precision has improved and what precision can be expected in general. These experiments are carried out both with and without pre-cooling of the CO_2.

Since the mass fraction of oil in typical cMQL applications is well below 1 % and the oil has no significant effect on the process cooling, all experiments to determine mass flow and cooling capacity as well as their dosing precision are performed without oil. In order to still obtain valid results for cMQL, the final experiments investigate how the pulsed application affects the oil output. For this purpose, a MQL oil and CO_2 are combined in the chair's own mixing system and fed to the nozzle together in one channel. The mixture is then applied in lines to blotting paper, which is weighed before and after application. While the CO_2 evaporates completely, the oil remains in the blotting paper. This allows the mass, the path width and the spray pattern of the oil application to be examined. The output of the smooth jet nozzles with continuous media application is again used as a reference. This is then compared with the pulsed output of the injector with nozzle diameter $d = 0.5$ mm at the same set output rate. The pulse frequencies are again $f_p = 50 / 100 / 150$ Hz and both room temperature CO_2 and pre-cooled CO_2 are used in this experiment. In each run, two lines are applied lengthwise to a DIN A4 sheet, see Fig. 3, at a feed speed of $v_f = 2000$ mm/min.

All the experiments described are repeated three times for statistical validation. The results presented in the upcoming chapter reflect the mean value of the three experiments. The standard deviation is not shown in the diagrams because it could not be displayed properly due to its small size. Control-specific parameters, especially regarding the energisation of the fuel injectors, are shown in Tab. 2.

Tab. 2: Control-specific parameters.

Dimension	Values
Pulse frequency f_p in Hz	50, 100, 150
Boost current I_b in A	7.0
Boost voltage U_b in V	60
Boost time t_b in µs	500
Holding current I_h in A	3.4
Holding voltage U_h in V	12
Holding time t_h in µs	variable

4 RESULTS

4.1 Maximum mass flow and cooling capacity

The results of the first experiment are shown in Fig. 4. As expected, the mass flow and the cooling capacity increase with increasing nozzle diameter. For a given nozzle diameter, all values with pre-cooled CO_2 exceed those of uncooled CO_2. For reference, pre-cooled CO_2 had a density of approximately $\rho = 865$ kg/m^3, while uncooled CO_2 had a density of approximately $\rho = 570$ kg/m^3. Without pre-cooling, there will be greater fluctuations of the density, however a sufficiently constant mass flow with corresponding cooling capacity is still achieved. With the exception of pre-cooled CO_2 and a nozzle diameter of $d = 0.3$ mm, the measured values lie on a curve that approaches a limit.

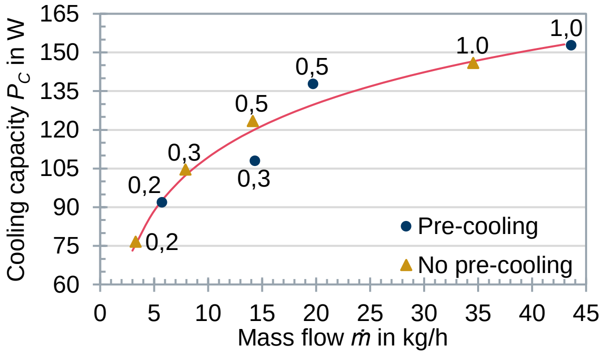

Fig. 4: Influence of nozzle diameter and pre-cooling on mass flow and cooling capacity.

For the smooth jet nozzles, the mass flow behaves as expected. Increasing the nozzle diameter from $d = 0.2$ mm to $d = 0.3$ mm increases the mass flow by a factor of approximately 2.25. For the used injectors the mass flow does not reach the theoretically predicted values. This becomes particularly clear at the transition from nozzle diameter $d = 0.5$ mm to $d = 1.0$ mm. Here a quadrupling of the mass flow is to be expected, which does not occur. When looking at the interior of the injector, it can be assumed that the internal geometry might limit the maximum flow and not only the nozzle diameter itself.

As the mass flow increases, the cooling capacity achieved flattens out significantly. There may be two reasons for this: On the one hand, this is due to the measuring principle. The heating resistor only provides a certain maximum heat output, above which stronger cooling is no longer measurable. This is most evident when using the injector with $d = 1.0$ mm, where a visible ice crystallisation forms on the surface of the heating resistor. On the other hand, parts of the CO_2 jet bounce off the heating resistor or flow past it, which is why they only contribute to cooling the heating resistor to a very small extent. Due to the stronger fanning out of the jet with larger nozzle diameters, this effect occurs more strongly with larger nozzle diameters.

As the mass flow and the cooling capacity of the smooth jet nozzles with $d = 0.2$ mm and $d = 0.3$ mm are to be reproduced in the following experiments, only the injector with $d = 0.5$ mm is used for this, as it can achieve this more efficiently than the injector with $d = 1.0$ mm. For the most efficient cooling of the process, it can therefore also be generally recommended that the nozzle diameter of the pulsed application is as close as possible to the nozzle diameter of the continuous application that it is intended to replace.

4.2 Initial dosing precision

To enable a comparison between the continuous and pulsed output in the following experiments, the continuous mass flows of the smooth jet nozzles with $d = 0.2$ mm and $d = 0.3$ mm are replicated by pulsed control of the injector with $d = 0.5$ mm. For this purpose, the maximum mass flow of the injector is reduced to a defined fraction at three different pulse frequencies. In this way, an equivalent mass flow can be set that corresponds to that of the smooth jet nozzles with $d = 0.2$ mm (0.2e) or $d = 0.3$ mm (0.3e). In these first characterisation experiments, it is still assumed that $t_o = t_h$, as shown in Formula (1). They are carried out again with pre-cooling (PC) and without pre-cooling (NPC).

Tab. 3 presents the fractions of the maximum mass flow of the injector with $d = 0.5$ mm for both nozzle equivalents and CO_2 states. It also lists the corresponding holding times for each frequency, calculated using Formula (1).

Tab. 3: Mass flow fractions and corresponding holding times depending on CO2 state and nozzle equivalent

Nozzle+CO_2 state	**Fraction of $\dot{m}_{max}$**	**t_h for 50 Hz**	**t_h for 100 Hz**	**t_h for 150 Hz**
0.2e-NPC	23.4 %	4675 µs	2335 µs	1555 µs
0.2e-PC	29.1 %	5820 µs	2910 µs	1940 µs
0.3e-NPC	55.9 %	11175 µs	5590 µs	3725 µs
0.3e-PC	72.7 %	14540 µs	7270 µs	4845 µs

Fig. 5 shows the comparison of continuous and pulsed application in terms of mass flow (left) and cooling capacity (right). The measured mass flow with mathematically equivalent pulsating output is slightly higher than the continuous output in all cases. In most cases, the discrepancy also increases slightly with increasing frequency. Both can be explained by the way in which the equivalent output is calculated. As described in chapter 3, the time period t_o during which the injector is at least partially open slightly exceeds the set holding time t_h.

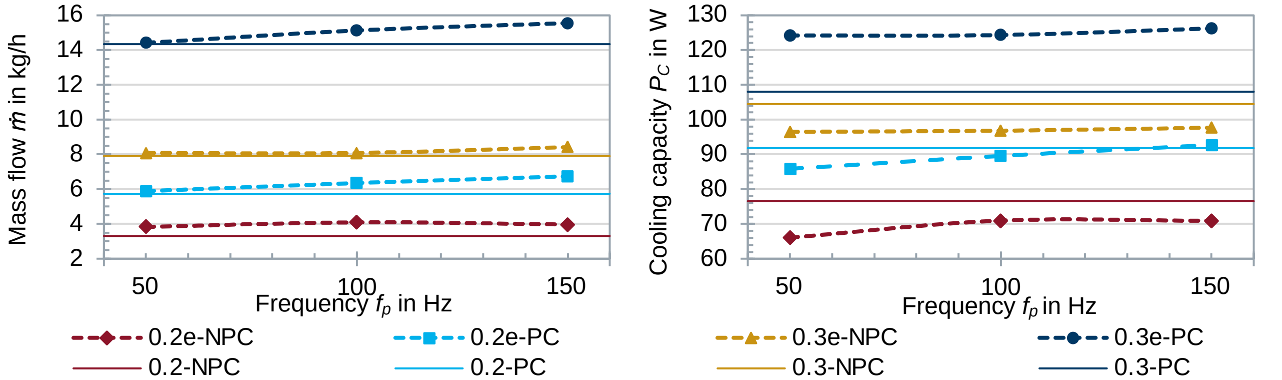

Fig. 5: Comparison of continuous and pulsed application in terms of mass flow and cooling capacity to determine the initial dosing precision.

The extended opening time per pulse results in an increased mass flow in general. Moreover, as the pulse frequency rises, the number of pulses per second increases, which further amplifies the deviation from the target mass flow. At the lowest frequency, the absolute deviation and thus the initial dosing accuracy of the mass flow ranges from 0.07 – 0.53 kg/h, at the medium frequency from 0.18 – 0.79 kg/h and at the highest frequency from 0.52 – 1.20 kg/h. This results in a corresponding relative deviation of 0.5 – 23.7 %.

The results for the cooling capacity appear more heterogeneous. However, the main reason for this lies in the measurement of the cooling capacity of the *d* = 0.3 mm nozzle with pre-cooled CO_2, which, as discussed in the previous chapter, is highly likely to be inaccurate. Therefore, this measurement is excluded from all following considerations. Excluding this measurement results in a coherent overall picture. The absolute deviation in cooling capacity ranges from 0.93 – 10.44 W, corresponding to a relative deviation of 1.0 – 13.6 %. With one exception, all measured values for pulsed application lie slightly below those of the continuous application. The reason for this is presumably the phenomenon already described. Due to the larger nozzle diameter of the injector with the same mass flow, a larger proportion of the CO_2 can only develop its cooling effect to a limited extent by bouncing off the heating resistor and flowing past it. The slight increase in cooling capacity over the frequency can probably be explained by the previously described increase in mass flow.

Fig. 6 shows the results from the previous figures combined to illustrate how the mass flow and cooling capacity are related in pulsed application and how they compare to continuous cooling.

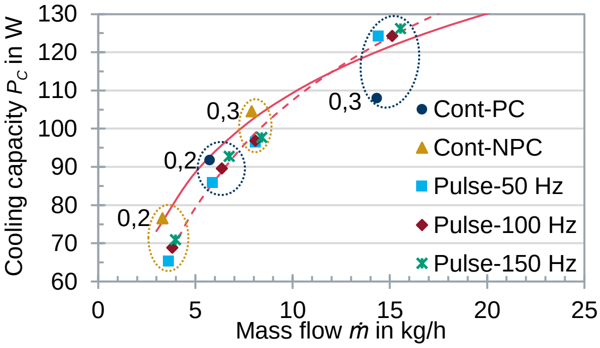

Fig. 6: Combined comparison of continuous and pulsed application in terms of mass flow and cooling capacity.

The continuous red trend line corresponds to that in Fig. 4. As already explained, the mass flow under pulsed feeding is slightly higher than in continuous mode, whereas the cooling capacity is slightly lower. For visualisation, a dashed trend line was added for the pulsed supply. This follows the continuous line but intersects it at a mass flow of $\dot m$ = 12 kg/h. In addition, clusters can be formed to assign the pulsed mass flows to the corresponding continuous mass flows. As already explained, the only outlier is the smooth jet nozzle with *d* = 0.3 mm.

4.3 Determination of the correction factor for the opening time

The results from section 4.2 show a deviation of up to 23.7 % between the measured and the targeted mass flow for pulsed feeding. As described in section 3.1 using Formula (2), this deviation most likely results from the time discrepancy $t_o > t_h$. Based on the measured maximum mass flow of the injector and the measured mass flow fraction from the initial dosing tests, the time deviation Δt can be determined using Formula (5).

$$\Delta t = \frac{\dot m_f}{f_p \cdot \dot m_{max}} - t_h \qquad (5)$$

To obtain a representative result, the average time deviation Δt is calculated across all three frequencies with their corresponding holding times, both with and without pre-cooling. For the used injector with a nozzle diameter of *d* = 0.5 mm, this yields an average deviation of Δt = 287 µs.

4.4 Validation experiments for dosing precision

The results of the validation tests to check the extended mathematical Formula (3) are shown in Fig. 7. As explained in section 3.2, the optimised holding times are calculated for the injector with nozzle diameter *d* = 0.5 mm at pulse frequencies of f_p = 50/150 Hz. These holding times were set to reach target mass flows of $\dot m$ = 5 kg/h (5-PC/5-NPC) and $\dot m$ = 10 kg/h (10-PC/10-NPC), respectively the experiments are again carried out with and without pre-cooling.

The maximum deviation between the aspired and measured mass flow is 0.38 kg/h absolute, corresponding to 7.6 % relative. This indicates a significantly improved dosing precision compared to the initial dosing tests, reducing the deviation to one third of its original value. In the experiments with pre-cooling, a slight increase in the mass flow is observed with increasing frequency, while the mass flow for the uncooled CO_2 remains constant. Nevertheless, the deviations from the target mass flow with uncooled CO_2 (0.27 – 0.38 kg/h) are somewhat greater than those with pre-cooled CO_2 (0.04 – 0.25 kg/h).

The expected cooling capacities derived from the dashed trend line in Fig. 6 (green lines in Fig. 7 on the right) are achieved for both set mass flows. The absolute deviations for the cooling capacity ranges from 0.32 – 3.31 W, thus to 0.3 – 4.2 % relative, which also equals one third of the previous deviations. Only at a mass flow of $\dot m$ = 5 kg/h does the measured cooling capacity rise slightly at a pulse frequency of f_p = 150 Hz. This confirms that not only the mass flow but also a corresponding cooling capacity can be set using the trend line in Fig. 6. Moreover, it demonstrates that the pulsed application can compensate for variations in CO_2 temperature and, consequently, CO_2 density.

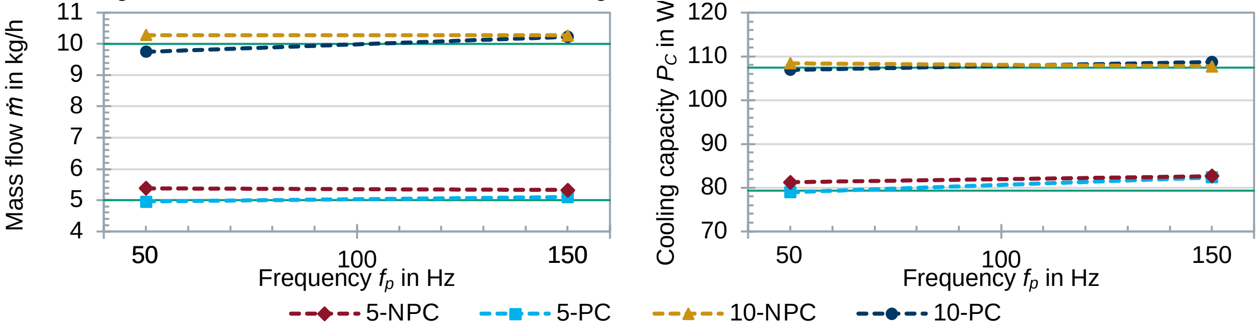

Fig. 7: Validation experiments in terms of mass flow and cooling capacity to determine the achievable dosing precision.

4.5 Effects of pulsed application on oil output

Spray tests were conducted on blotting paper to evaluate the oil discharge during pulsed application. Fig. 8 shows the applied oil quantities as a function of CO_2 mass flow, with the oil discharge of the smooth jet nozzles indicated directly in the graph. Greater fluctuations in mass flow are observed, particularly for uncooled CO_2. This is likely due to larger density fluctuations and an overall lower density, which suggests that the proportion of the gaseous phase of the CO_2 in the riser bottle bundle is increasing. Nevertheless, the average mass flow for uncooled CO_2 remains within the range of the previously conducted experiments. For pre-cooled CO_2, the mass flow rates are constant, although they are below the expected values from the dosing tests.

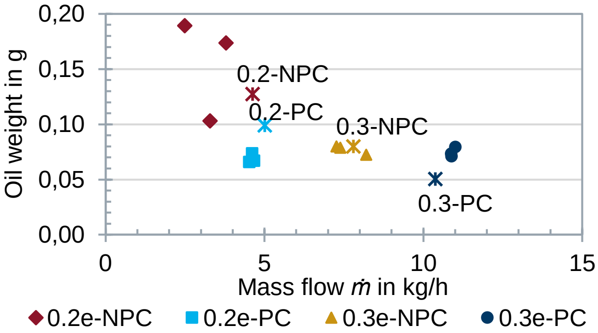

Fig. 8: Applied oil weight as a function of mass flow for continuous and pulsed cMQL.

The applied oil quantity varies, particularly for the 0.2e-NPC. At a low and fluctuating mass flow, oil is applied irregularly, resulting in an increased oil weight. This may be due to oil accumulating in the piping system during the phases of low CO_2 flow, which is then expelled in concentrated form once sufficient CO_2 flow resumes. However, for the 0.3e-NPC the measured oil weight is comparable to that of the continuous application using the smooth jet nozzle. Except for the 0.2e-NPC, pulsed application results in largely consistent oil quantities, regardless of the mass flow. In contrast, during continuous application with the smooth jet nozzles, the oil weight decreases as the CO_2 mass flow increases. Compared to continuous application, the pulsed application results in a lower oil quantity for the 0.2e-PC and a higher quantity for the 0.3e-PC.

The widths of the spray paths are shown in Fig. 9 as a function of the CO_2 mass flow. There is an increase in the width of the spray path with increasing mass flow for both continuous and pulsed application.

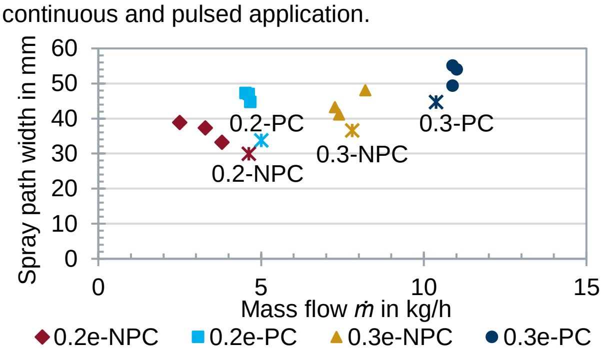

Fig. 9: Spray path width as a function of mass flow for continuous and pulsed cMQL.

In addition, the measured spray paths of the injector with $d = 0.5$ mm are consistently larger than those of the two smooth jet nozzles with $d = 0.2$ mm and $d = 0.3$ mm. Both observations are related to the expansion of the CO_2-oil jet after leaving the nozzle. This is due to the increased CO_2 mass flow and the larger nozzle diameter, both of which promote a wider jet expansion [Gross 2021].

Fig. 10 shows some examples of the applied oil streaks with pre-cooled CO_2, with one square corresponding to one centimetre. The spray paths of the smooth jet nozzle with $d = 0.2$ mm have a comparatively narrow but intense strip in the centre with a width of 1 cm. The pulsed application of the 0.2e with pre-cooling, on the other hand, results in a wider but very uniform application of oil. Without pre-cooling, however, the oil application of the 0.2e is rather irregular, both along and across the feed direction.

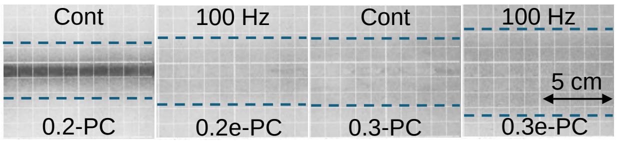

Fig. 10: Exemplary oil streaks applied to blotting paper.

The width of the oil spray paths for the smooth jet nozzle with $d = 0.3$ mm is greater than those of the nozzle with $d = 0.2$ mm but varies depending on whether the CO_2 is pre-cooled or not. Without pre-cooling there is a lower mass flow and therefore a slightly narrower application with a thin, more intense streak in the centre. In contrast, the mass flow is greater with pre-cooling, resulting in a wider spray path. In the centre, however, there is a pale streak with reduced oil application. The pulsed application of the 0.3e is again wider than the continuous application due to the larger nozzle diameter of $d = 0.5$ mm. In addition, the distribution both along and across the feed direction is more uniform than without pulsation. This uniformity manifests itself particularly in less pronounced streaks in the centre of the path.

To summarise, it can be said that oil application with the HFpcMQL already works well, achieving a uniform oil application. However, it should be noted that, as expected, the spray path width also increases due to the larger nozzle diameter of the injector. In addition, a consistent mass flow is essential for uniform oil application. If the mass flow is low and irregular, oil may accumulate in the pipe system, leading to an unsteady spray pattern.

5 CONCLUSION AND OUTLOOK

In the present paper, the behaviour of CO_2-based HFpcMQL was examined and compared with continuous cMQL. Questions regarding the dosing precision of mass flow and cooling capacity, the possibility of compensating the CO_2 input quality and the oil output were investigated. The following conclusions were drawn:

- The maximum mass flow and the associated cooling capacity depend on the nozzle diameter and CO_2 density. The cooling capacity measured flattens out as the mass flow increases, but this is due to the measuring principle used on one hand and presumably the CO_2 bouncing off and flowing past the heating resistor on the other hand. The mass flow is also influenced by the interior of the injector. This must be considered when selecting injectors for use in the HFpcMQL.
- For maximum efficiency, the nozzle diameter of modified injectors should generally be as close as possible to the nozzle diameter of the continuous application that is to be substituted.
- Even without improved dosing precision, the high-frequency pulsed application can be used to adjust the mass flow and cooling capacity. The absolute deviation from the target values for the mass flow was between 0.07 – 1.20 kg/h, which corresponds to a relative

deviation of 0.5 – 23.7 %. For the cooling capacity it was 0.93 – 10.44 W, corresponding to 1.0 – 13.6 %.

- To improve the dosing accuracy, a correction factor of Δt = 287 µs was calculated for the specific injector used. This corresponds to the time in which the injector is theoretically fully open before and after the holding time, while the actual time the injector is at least partially open is even longer.
- After taking the correction factor into account, the mass flow dosing precision improved to 0.04 – 0.38 kg/h absolute, corresponding to 0.08 – 7.6 % relative. The absolute deviation for the cooling capacity was 0.32 – 3.31 W, thus to 0.3 – 4.2 % relative.
- The experiments show that the cooling capacity depends almost exclusively on the mass flow of the CO_2 as long as it remains mainly in the liquid state. Since the mass flow can be precisely adjusted by the system presented, even with uncooled CO_2 of lower density, it is therefore also possible to provide the cutting zone with a selected cooling capacity – regardless of the liquid CO_2 density.
- A minimum mass flow of CO_2 is required for uniform oil entrainment. If this condition is not met, oil may collect in the feed lines, which is then ejected in lumps.
- The path width of the oil application depends on the nozzle diameter and the mass flow. However, the size of the sprayed area should be adjustable by modifying the distance to the cutting zone [Gross 2021].
- As already mentioned, uniform oil application requires a minimum mass flow of CO_2. If this is ensured, a uniform spray pattern can be achieved with both the jet nozzles and the high-frequency pulsed application. This applies equally to all frequencies analysed.

With the system presented, both high-frequency pulsed and continuous application of cMQL can be considered almost equivalent, at least outside the machining process. The next step will be to investigate whether these results can also be confirmed during the actual machining process.

6 ACKNOWLEDGMENTS

This paper is part of the research for the 'KryoPuls' project, funded by the 'Bayerische Forschungsstiftung'.

7 REFERENCES

[Bagherzadeh 2018] Bagherzadeh, A. and Budak, E. Investigation of machinability in turning of difficult-to-cut materials using a new cryogenic cooling approach. Tribology International, 2018, Vol. 119, pp 510-520

[Biermann 2015] Biermann, D., et al. Experimental investigation of tool wear and chip formation in cryogenic machining of titanium alloys. Adv. Manuf., 2015, Vol.3, pp 292-299

[Degner 2019] Degner, W., et al. Spanende Formung. München: Carl Hanser Verlag, 2019. ISBN 9783446460638

[Denkena 2011] Denkena, B. and Tönshoff, H.K. Spanen: Grundlagen. Berlin: Springer Verlag, 2011. ISBN 9783642197710

[Gross 2021] Gross, D. Untersuchungen zur kohlenstoffdioxidbasierten kryogenen Minimalmengenschmierung. FAU Studien aus dem Maschinenbau Band 365. Erlangen: FAU University Press, 2021.

[Gupta 2023] Gupta, M.K., et al. Potential use of cryogenic cooling for improving the tribological and tool wear characteristics while machining aluminium alloys. Tribology International, 2023, Vol. 183, pp 108434

[Hanenkamp 2018] Hanenkamp, N., et al. Hybrid Supply System for Conventional and CO_2/MQL-based Cryogenic Cooling. Procedia CIRP, 2018, Vol. 77, pp 219-22

[Hong 2000] Hong, S.Y. and Broomer, M. Economical and ecological cryogenic machining of AISI 304 austenitic stainless steel. Clean Products and Processes, 2000, Vol.2, pp 157-166

[Howes 1991] Howes, T.D., et al. Environmental Aspects of Grinding Fluids. CIRP Annals, 1991, Vol.40, No.2, pp 623-630

[Iruj 2024] Iruj, M., et al. State-of-the-art hybrid lubrication (Cryo-MQL) supply systems, performance evaluation, and optimization studies in various machining processes. Results in Engineering, 2024, Vol.22, pp 102090

[Iqbal 2023] Iqbal, A., et al. Side-milling of Incoloy 825 under pulsed and continuous modes of cryogenic cooling. Journal of Manufacturing Processes, 2023, Vol.104, pp 246-256

[Iqbal 2024] Iqbal, A., et al. Investigations on pulsed and continuous supply of a cryogenic medium in milling of Waspaloy and Inconel 718 under various lubri-cooling environments. Int J Adv Manuf Technol, 2024, Vol.132, pp 3027-3046

[Jerold 2012] Jerold, B.D. and Kumar, M.P. Machining of AISI 316 Stainless Steel under Carbon-Di-Oxide Cooling. Materials and Manufacturing Processes, 2012, Vol.27, No.10, pp. 1059-1065

[Kißler 2004] Kißler, H. Trockenbearbeitung in der Praxis. Stuttgart: Landesgewerbeamt Baden-Württemberg Informationszentrum für betrieblichen Umweltschutz, 2004

[Klocke 2008] Klocke, F. and König, W. Fertigungsverfahren 1: Drehen, Fräsen, Bohren. Berlin: Springer, 2008. ISBN 978-3-540-23458-6

[Meier 2024] Meier, T., et al. Investigation of the effects of CO_2 pre-cooling on the cooling capacity for cryogenic cooling in machining operations. CIRP Journal of Manufacturing Science and Technology, 2024, Vol.55, pp 88-97

[Naik 2023] Naik, D.N.S. and Sharma, V. Development of pulse-assisted cryo-micro lubrication architecture for machining of Ti-based alloys: A frugal innovative attempt for a hybrid lubri-cooling technique. Journal of Manufacturing Processes, 2023, Vol.91, pp 61-77

[Najiha 2016] Najiha, M.S., et al. Environmental impacts and hazards associated with metal working fluids and recent advances in the sustainable systems: A review. Renewable and Sustainable Energy Reviews, 2016, Vol.60, pp 1008-1031

[NIOSH 1998] National Institute for Occupational Safety and Health. Criteria for a recommended standard: Occupational exposure to metalworking fluids. Cincinnati: U.S. Department of Health and Human Services, 1998

[Pimenov 2024] Pimenov, D.Y., et al. A comprehensive review of machinability of difficult-to-machine alloys with advanced lubricating and cooling techniques. Tribology International, 2024, Vol.196, pp 109677

[Stephenson 2014] Stephenson, D. A., et al. Rough turning Inconel 750 with supercritical CO_2-based minimum quantity lubrication. Journal of Materials Processing Technology, 2014, Vol.214, pp 673-680

[Villarrazo 2023] Villarrazo, N., et al. The Effects of Lubricooling Ecosustainable Techniques on Tool Wear in Carbon Steel Milling. Materials, 2023, Vol.16, pp 2936

[Wang 2000] Wang, Z.Y. and Rajurkar, K.P. Cryogenic machining of hard-to-cut materials. Wear, 2000, Vol.239, pp 168-175